Latency Minimization for Wireless Powered Mobile Edge Computing Networks With Nonlinear Rectifiers

Junhee Park, Sourabh Solanki, *Member, IEEE*, Seunghwan Baek, and Inkyu Lee, *Fellow, IEEE*

***Abstract*—This paper investigates a wireless powered mobile edge computing (MEC) network where a hybrid access point (H-AP) serves energy-constrained devices. For such a wireless powered MEC network, the H-AP first transmits wireless information and energy simultaneously in the downlink. Then, by utilizing the harvested energy, the device processes both its local data and the received data from the H-AP. In this system, we minimize the latency by jointly optimizing the power splitting ratio of rectifiers, the data offloading power, the local computing frequency, and the data offloading ratio at the device. By applying a polyblock outer approximation procedure, we propose an algorithm which guarantees the optimal solution. Simulation results verify the efficiency of the proposed algorithm compared to conventional schemes.**

***Index Terms*—Mobile edge computing, wireless power transfer, latency minimization.**

I. Introduction

Recently, mobile edge computing (MEC) systems have attracted great attentions [1], which exploit vast resource available on a central server for executing the task of end users. The MEC system has been regarded as a promising solution for wireless networks consisting of latency-critical and energy-constrained devices such as internet-of-things (IoT) sensors [2]–[7]. In the MEC system, the central server can provide users with rapid and energy efficient data processing capabilities which facilitate data offloading. Compared to full offloading strategies where data computing is entirely executed at the server, the partial offloading technique allows data computing to be performed both in a server and a user terminal so that their computation resources can be utilized more efficiently [2].

On the other hand, it is well established that radio frequency (RF) signals can transport data and energy simultaneously [8]. As a consequence, RF-based wireless power transfer protocols have been considered in many traditional wireless network scenarios [9]–[22]. Particularly, in [11], a simultaneous wireless information and power transmission (SWIPT) network was investigated where a hybrid access point (H-AP) sends information and energy simultaneously to receivers with the aim of maximizing the harvested energy. To support concurrent information decoding (ID) and energy harvesting (EH) operations at the receivers, time switching and power splitting architectures were studied in [12]. The works in [13], [14] investigated the implementation issues and provided experimental analysis of the receiver design problems to realize the SWIPT architectures. Owing to its potential of charging devices without battery replacements, energy can be provided to energy-limited devices in indoor IoT platform or vehicular-to-everything (V2X) networks [7]. Accordingly, the application of wireless power transfer techniques to the MEC network has been studied in the recent literature [15]–[18]. In practical EH circuits, the harvested power varies nonlinearly with the input power such that it becomes saturated at a high input power region. To characterize such a behaviour of EH circuits, authors in [19] introduced a practical nonlinear EH model based on measurement data. By adopting this model, nonlinear rectifiers based EH receiver designs were presented in [20]–[22] for various wireless network scenarios.

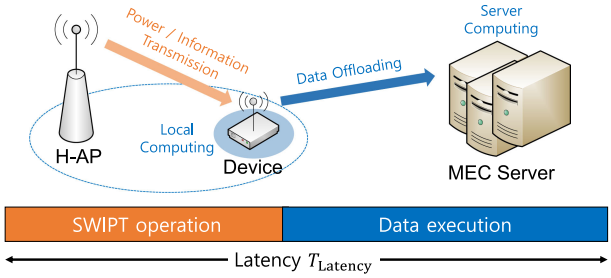

Fig. 1. Schematic diagram of wireless powered MEC networks.

In this work, we investigate wireless powered MEC networks combined with SWIPT techniques where an H-AP supports an energy-constrained device equipped with multiple nonlinear EH rectifiers. Specifically, to overcome the saturation issue in the nonlinear EH model which has not been fully investigated in the existing works [16], [17], we have adopted the multiple EH rectifiers structure in [20]. By employing multiple rectifiers, the device is able to avoid the operation in the saturation region, which, in turn, enhances wireless power transfer efficiency. Furthermore, utilizing the harvested energy, the device executes the data computation under a partial offloading strategy where a portion of the data is offloaded to a MEC server while the remaining data is locally computed at the device. With such a partial offloading policy, the harvested energy can be effectively and flexibly allocated to the local computing and the data offloading processes for reducing the computation latency of energy-limited devices. To the best of the authors' knowledge, existing literatures related to wireless powered MEC systems have not addressed the saturation issue and its solution.

To fully exploit the advantage of the proposed structure, we focus on the latency minimization by jointly optimizing the power splitting ratio at each EH circuit, the data offloading power to the MEC server, the local computing frequency, and the data offloading ratio of data at the device. Since the resulting problem is generally nonconvex and complex, it is challenging to find the optimal solution. Therefore, based on the polyblock outer approximation framework [23], we propose an efficient algorithm that guarantees the global optimal solution. It is emphasized that such an optimization solution in the context of wireless powered MEC networks has not been reported before in the literature. Then, simulation results demonstrate that the proposed joint optimization algorithm can substantially reduce the latency of the wireless powered MEC network.

II. System Model and Problem Formulation

As shown in Fig. 1, we consider an MEC network where a single antenna device, which contains X_{L} amount of local data (in bits), is supported by an H-AP. In the network, the H-AP first transmits the RF signal to the device during the downlink SWIPT time T_{S} (in seconds) for sending X_{C} amounts of data, and charging the battery simultaneously. The data X_{C} can convey control messages or information acquired at other devices as in [15]. It is assumed that the device has N_{rec} rectifiers and employs a power splitting strategy where ρ_{ID} portion of the received power is allocated to ID while the remaining $1-\rho_{\text{ID}}$ is assigned to

Manuscript received May 20, 2020; revised November 10, 2020 and March 31, 2021; accepted June 25, 2021. Date of publication June 30, 2021; date of current version August 13, 2021. This work was supported by the National Research Foundation of Korea (NRF) grant funded by the Korea government (MSIT) under Grant 2017R1A2B3012316. The review of this article was coordinated by Dr. Berk Canberk. *(Corresponding author: Inkyu Lee.)*

The authors are with the School of electrical engineering, Korea University, Seoul 02841, South Korea (e-mail: pjh0585@korea.ac.kr; sourabhsolanki@ieee.org; s_baek@korea.ac.kr; inkyu@korea.ac.kr).

Digital Object Identifier 10.1109/TVT.2021.3093630

the rectifiers for the EH operation. As such, the $1-\rho_{\text{ID}}$ portion of the power is further subdivided among N_{rec} rectifiers. In other words, the power assigned for the EH is given as $1-\rho_{\text{ID}}=\sum_{n=1}^{N_{\text{rec}}}\rho_n$ where ρ_n represents the fraction of power dedicated to the n-th rectifier for $n\in\mathcal{N}=\{1,..,N_{\text{rec}}\}$.

Then, the downlink SWIPT time T_{S} with respect to ρ_{ID} is written as

$$T_{\text{S}}(\rho_{\text{ID}})=\frac{X_{\text{C}}}{B\log_2\left(1+\frac{|h_{\text{D}}|^2P_{\text{D}}}{\sigma^2}\rho_{\text{ID}}\right)}, \tag{1}$$

where B, h_{D}, P_{D}, and σ^2 stand for the channel bandwidth, the downlink channel gain between the H-AP and the device, the transmission power of the H-AP, and the noise variance at the device, respectively. To be specific, the denominator in equation (1) represents the achievable downlink transmission rate from the H-AP to the device. Also, based on the nonlinear EH model [19], the total harvested power during $T_{\text{S}}(\rho_{\text{ID}})$ at the device can be expressed as

$$P_{\text{har}}=\sum_{n=1}^{N_{\text{rec}}}\frac{M_{\max}}{1-\Omega}\left(\frac{1}{1+\exp\left(-a(|h_{\text{D}}|^2P_{\text{D}}\rho_n-b)\right)}-\Omega\right), \tag{2}$$

where $M_{\max}$ indicates the maximum saturated harvesting power, and a, b, and $\Omega=1/(1+e^{ab})$ are determined by the circuit specifications of each rectifier.

To compute the data $X_{\text{T}}=X_{\text{L}}+X_{\text{C}}$ with the harvested energy, it is assumed that the total data is processed by parallel computing [16], [18]. Specifically, the device offloads β portion of the data, i.e., βX_{T}, to the server. After the server completes the computation, the results are sent back to the device. In the meantime, the remaining $1-\beta$ portion of the data, i.e., $(1-\beta)X_{\text{T}}$, is locally computed at the device. Thus, under the dynamic voltage scaling (DVS) model [2], the local computing time T_{LC} at the device and the offloading time T_{DO} of the task at the device can be obtained, respectively, as

$$T_{\text{LC}}=\frac{c(1-\beta)X_{\text{T}}}{f_{\text{LC}}},\quad T_{\text{DO}}=\frac{\beta X_{\text{T}}}{B\log_2(1+\frac{|h_{\text{U}}|^2}{\sigma^2}P_{\text{U}})}, \tag{3}$$

where c, f_{LC}, h_{U}, and P_{U} denote the number of the required central processing unit (CPU) cycles per bit, the local computing frequency of the device's CPU in cycles per second, the uplink channel gain between the device and the MEC server, and the transmission power of the device, respectively. Also, we adopt the channel model $|h_i|^2=d_i^{-l}g_i|\bar{h_i}|^2$ for $i\in\{\text{D},\text{U}\}$ where l, g_i, d_D and d_U indicate the path-loss exponent, the reference path-loss, the distance between the H-AP and the device, and between the device and the MEC server, respectively, and $\bar{h_i}\in\mathbb{C}$ represents the normalized channel fading coefficient.

We assume that the power resource of the server is relatively high with respect to the device and the output size is small.[1] Therefore, in the following formulation, the computing time at the server and the downlink transmission time of the output are neglected as in [18]. As a result, under the partial offloading strategy with parallel computing, we can define the data execution time as $T_{\text{DE}}=\max(T_{\text{LC}},T_{\text{DO}})$ and the total latency in the wireless powered MEC network is given as $T_{\text{latency}}=T_{\text{S}}(\rho_{\text{ID}})+T_{\text{DE}}$.

In this paper, we aim to minimize the latency T_{latency} by jointly optimizing the power splitting ratios ρ_{ID} and $\{\rho_n\}$, the data offloading ratio β, the local computing frequency f_{LC}, and the data offloading power P_{U} at the device. The latency minimization problem can be formulated as

$$(\text{P}):\min_{\rho_{\text{ID}},\{\rho_n\},\beta,f_{\text{LC}},P_{\text{U}}}\quad T_{\text{latency}}$$

$$\text{s.t. }\frac{T_{\text{S}}(\rho_{\text{ID}})}{X_{\text{T}}}(P_{\text{har}}-P_{\text{o}})\geq\kappa c(1-\beta)f_{\text{LC}}^2+\frac{\beta P_{\text{U}}}{B\log_2(1+\frac{|h_{\text{U}}|^2P_{\text{U}}}{\sigma^2})}, \tag{4}$$

$$0<\rho_{\text{ID}}<1, \tag{5}$$

$$\rho_{\text{ID}}+\sum_{n=1}^{N_{\text{rec}}}\rho_n=1,\ \text{and}\ \ \rho_n\geq 0,\ \text{for}\ n\in\mathcal{N}, \tag{6}$$

$$0\leq\beta\leq 1, 0\leq f_{\text{LC}}\leq f_{\text{LC}}^{\text{M}}, 0\leq P_{\text{U}}\leq P_{\text{U}}^{\text{M}}, \tag{7}$$

where κ and P_{o} represent the coefficient related to the chip architecture [2] and the power consumed for the device's on-board processing, which is assumed to be sufficiently small, and f_{LC}^{M} and P_{U}^{M} indicate the maximum computing frequency and the peak offloading power at the device, respectively. The first term in the right hand side of the energy causality constraint (4) is the required energy per bit for the local computing, while the second term accounts for the data offloading. The constraint in (6) ensures that the received power is split into ρ_{ID} portion of the ID operation and ρ_n portion for the n-th EH rectifier. Note that (P) includes both the local computing without offloading and the full offloading schemes as special cases with $\beta=0$ and 1, respectively. It can be checked that the objective and the constraint in (4) are nonconvex functions which cannot be handled easily.

To deal with this nonconvex problem, we first reformulate (P) by applying the change of variable $R_{\text{U}}=\log_2(1+\frac{|h_{\text{U}}|^2}{\sigma^2}P_{\text{U}})$. Then, the data execution time T_{DE} can always be reduced by adjusting β to satisfy $T_{\text{LC}}=T_{\text{DO}}$ without violating the constraint in (4). Therefore, the optimal data offloading ratio β for other given variables can be derived as $\beta^*=\frac{BR_{\text{U}}}{\frac{f_{\text{LC}}}{c}+BR_{\text{U}}}$. After plugging β^* into (P), (P) can be reformulated as

$$(\text{P}'):\min_{\rho_{\text{ID}},\{\rho_n\},f_{\text{LC}},R_{\text{U}}}\quad T_{\text{S}}(\rho_{\text{ID}})+\frac{X_{\text{T}}}{\frac{1}{c}f_{\text{LC}}+BR_{\text{U}}}$$

$$s.t.\ \frac{T_{\text{S}}(\rho_{\text{ID}})}{X_{\text{T}}}(P_{\text{har}}-P_{\text{o}})\geq\frac{\kappa f_{\text{LC}}^3+\frac{\sigma^2}{|h_{\text{U}}|^2}(2^{R_{\text{U}}}-1)}{\frac{1}{c}f_{\text{LC}}+BR_{\text{U}}}, \tag{8}$$

$$0\leq f_{\text{LC}}\leq f_{\text{LC}}^{\text{M}},\ 0\leq R_{\text{U}}\leq R_{\text{U}}^{\text{M}},$$

$$(5),(6), \tag{9}$$

where $R_{\text{U}}^{\text{M}}\triangleq\log_2(1+\frac{|h_{\text{U}}|^2}{\sigma^2}P_{\text{U}}^{\text{M}})$.

It is still not straightforward to determine the globally optimal solution in (P′) due to the nonconvex constraint (8). In the following section, we present an efficient approach for solving (P′).

III. Proposed Algorithm for Latency Minimization

A. Maximization of Harvested Power

To tackle the problem (P′), we first maximize the harvested power P_{har} in constraint (8) by optimizing the EH power splitting ratio $\{\rho_n\}$ as a function of ρ_{ID}. By introducing auxiliary variables P_{in} and $\{\delta_n\}$ and applying the change of variable $P_{\text{in}}=|h_{\text{D}}|^2P_{\text{D}}(1-\rho_{\text{ID}})$ and $\rho_n=\frac{1}{P_{\text{in}}}\log(1+\delta_n)$ for $n\in\mathcal{N}$, the harvested power maximization problem can be written as

$$\max_{\{\delta_n\geq 0\}}\ F_1(\{\delta_n\})\triangleq\sum_{n=1}^{N_{\text{rec}}}\frac{1}{1+\frac{\exp(ab)}{1+\delta_n}}$$

$$s.t.\ \sum_{n=1}^{N_{\text{rec}}}\log(1+\delta_n)\leq aP_{\text{in}}. \tag{10}$$

It can be checked that this problem is nonconvex as the constraint is not convex. However, the optimal solution of the problem can be obtained

[1]This assumption is valid in wireless sensor networks with IoT devices [16], [18].

from one of the Karush-Kuhn-Tucker points [24]. First, the Lagrangian of the above problem is given as

$$\mathcal{L}_1(\{\delta_n\},\lambda_0,\{\lambda_n\}) \triangleq - F_1(\{\delta_n\}) + \lambda_0\left(\sum_{n=1}^{N_{\text{rec}}}\frac{\log(1+\delta_n)}{aP_{\text{in}}} - 1\right) - \sum_{n=1}^{N_{\text{rec}}}\lambda_n\delta_n, \quad (11)$$

where λ_n for $n \in \{0,1,\ldots,N_{\text{rec}}\}$ represents nonnegative dual variables, and the stationary condition states that

$$\lambda_n = \frac{\lambda_0}{aP_{\text{in}}(1+\delta_n)} - \frac{e^{ab}}{(e^{ab}+1+\delta_n)^2}, \text{ for } n \in \mathcal{N}. \quad (12)$$

By the complementary slackness condition $\lambda_n\delta_n = 0$ for $n \in \mathcal{N}$, we can induce that the rectifiers are separated into two disjoint sets, which are defined as $\mathcal{N}_1 = \{n \in \mathcal{N} | \delta_n = 0\}$ and $\mathcal{N}_2 = \{n \in \mathcal{N} | \delta_n \neq 0\}$ with $\mathcal{N}_1 \cup \mathcal{N}_2 = \mathcal{N}$. Then, all possible sets of $\mathcal{N}_1$ and $\mathcal{N}_2$ can be the candidates of the optimal set of indices corresponding to the optimal solution $\{\delta_n^*\}$. Since $\lambda_n = 0$ for $n \in \mathcal{N}_2$ by the complementary slackness, the corresponding δ_n satisfies

$$\lambda_0 = \frac{aP_{\text{in}}e^{ab}(1+\delta_n)}{(e^{ab}+1+\delta_n)^2}, \text{ for } n \in \mathcal{N}_2. \quad (13)$$

Also, it can be found that the equality in constraint (10) should hold since $\lambda_0 > 0$. As a result, without loss of generality, the optimal EH power splitting solution can be derived as

$$\rho_n^* = \begin{cases} \frac{1-\rho_{\text{ID}}}{N^*}, & \text{for } n = 1,\ldots,N^*, \\ 0, & \text{for } n = N^*+1,\ldots,N_{\text{rec}}, \end{cases} \quad (14)$$

where N^* is expressed by

$$N^* = \arg\max_{N\in\{1,\ldots,N_{\text{rec}}\}} \frac{N}{1+\exp\left(-a(\frac{P_{\text{in}}}{N}-b)\right)}. \quad (15)$$

This means that the optimal EH power splitting solution $\{\rho_n^*\}$ is assigned identically for N^* rectifiers where N^* is determined by P_{in}, which is a function of ρ_{ID}. Based on (14), for a given ρ_{ID}, the maximum harvested power $P_{\text{har}}^*(\rho_{\text{ID}})$ is computed as

$$P_{\text{har}}^*(\rho_{\text{ID}}) = \frac{N^*M_{\max}}{1-\Omega}\left(\frac{1}{1+\exp\left(-a(\frac{P_{\text{in}}}{N^*}-b)\right)} - \Omega\right). \quad (16)$$

From (16), it can be noted that $P_{\text{har}}^*(\rho_{\text{ID}})$ is a decreasing function with respect to ρ_{ID} since P_{in} is a linear function of ρ_{ID}. Next, in the following subsection, by using the result in (16), the optimal local computing frequency f_{LC}^* and the data offloading rate R_{U}^* are derived as a function of ρ_{ID}.

B. Minimization of Computation Latency

For a given ρ_{ID}, (P′) can be reduced to

$$\max_{f_{\text{LC}},R_{\text{U}}} \quad F_2(f_{\text{LC}},R_{\text{U}}) \triangleq f_{\text{LC}} + cBR_{\text{U}}$$

$$s.t.\ \ \kappa c f_{\text{LC}}^3 + \tfrac{c\sigma^2}{|h_{\text{U}}|^2}(2^{R_{\text{U}}}-1) \le C(\rho_{\text{ID}})(f_{\text{LC}} + cBR_{\text{U}}), \quad (17)$$

$$0 \le f_{\text{LC}} \le f_{\text{LC}}^M,\ \ 0 \le P_{\text{U}} \le P_{\text{U}}^M, \quad (18)$$

where $C(\rho_{\text{ID}}) = \frac{X_{\text{C}}}{X_{\text{T}}}T_{\text{S}}(\rho_{\text{ID}})(P_{\text{har}}^*(\rho_{\text{ID}}) - P_{\text{o}})$. Since this problem is convex and satisfies the Slater's condition, the optimal solution can be obtained by the Lagrangian duality method.

The dual function of the above problem can be written as

$$\mathcal{G}(\{\nu_j\}) = \min_{f_{\text{LC}},R_{\text{U}}} \mathcal{L}_2(f_{\text{LC}},R_{\text{U}},\{\nu_j\}), \quad (19)$$

where

$$\mathcal{L}_2(f_{\text{LC}},R_{\text{U}},\{\nu_j\}) \triangleq -F_2(f_{\text{LC}},R_{\text{U}}) + \nu_0\left(\kappa c f_{\text{LC}}^3 + \tfrac{c\sigma^2}{|h_{\text{U}}|^2}(2^{R_{\text{U}}}-1) - C(\rho_{\text{ID}})(f_{\text{LC}} + cBR_{\text{U}})\right) + \nu_1(f_{\text{LC}} - f_{\text{LC}}^M) + \nu_2(R_{\text{U}} - R_{\text{U}}^M), \quad (20)$$

and $\{\nu_j\}$ for $j = 0,1,2$ represent nonnegative dual variables corresponding to the constraints in (17) and (18).

By taking the derivative of (20) with respect to f_{LC} and R_{U}, we have

$$\nu_1 = 1 - \nu_0\left(3\kappa c f_{\text{LC}}^2 - C(\rho_{\text{ID}})\right), \quad (21)$$

$$\frac{1}{cB}\nu_2 = 1 - \nu_0\left(\log 2 \frac{\sigma^2}{|h_{\text{U}}|^2 B}2^{R_{\text{U}}} - C(\rho_{\text{ID}})\right). \quad (22)$$

Then, the complementary slackness condition yields the optimal solution f_{LC}^* and R_{U}^* as

$$f_{\text{LC}}^* = \min\left(\sqrt{\frac{1}{3\kappa c}(C(\rho_{\text{ID}})+\mu)}, f_{\text{LC}}^M\right), \quad (23)$$

$$R_{\text{U}}^* = \min\left(\left[\log_2\frac{|h_{\text{U}}|^2 B}{\sigma^2\ln 2}(C(\rho_{\text{ID}})+\mu)\right]^+, R_{\text{U}}^M\right), \quad (24)$$

where $\mu \triangleq 1/\nu_0$ satisfies

$$\kappa(f_{\text{LC}}^*)^3 + \tfrac{\sigma^2}{|h_{\text{U}}|^2}\left(2^{R_{\text{U}}^*}-1\right) - C(\rho_{\text{ID}})\left(\tfrac{1}{c}f_{\text{LC}}^* + BR_{\text{U}}^*\right) = 0, \quad (25)$$

and $[x]^+$ is defined as $\max(x,0)$.

It can be easily shown that by taking the derivative, equation (25) is increasing with respect to μ for a fixed ρ_{ID}. Therefore, μ can be obtained by a bisection search method. Note that the optimal data offloading ratio can be written as

$$\beta^* = \frac{BR_{\text{U}}^*}{\frac{f_{\text{LC}}^*}{c} + BR_{\text{U}}^*}, \quad (26)$$

as mentioned in Section II. Also, since both $C(\rho_{\text{ID}})$ and μ are decreasing functions with respect to $\rho_{\text{ID}} \in (0,1)$, we can see that both f_{LC}^* and R_{U}^* are nonincreasing with respect to ρ_{ID} by checking the subgradient of (23) and (24). Here, the proofs are omitted for brevity.

C. Proposed Optimum Algorithm

In the previous subsections, we have derived the optimal EH power splitting ratio $\{\rho_n^*\}$, the local computing frequency f_{LC}^*, and the data offloading rate R_{U}^*. Note that since all the optimization variables are expressed as a function of ρ_{ID}. After plugging (14), (23), and (24) into (P′) and introducing a slack variable ω, we can rewrite the original problem (P) as

$$(\text{P}'') : \max_{\rho_{\text{ID}},\omega} \quad F_3(\rho_{\text{ID}},\omega) \triangleq -\left(T_{\text{S}}(\rho_{\text{ID}}) + \frac{X_{\text{L}}+X_{\text{C}}}{\omega}\right)$$

$$s.t.\ \omega + G(\rho_{\text{ID}}) \le 0, \quad (27)$$

$$0 \le \rho_{\text{ID}} \le 1,\ \omega \ge 0, \quad (28)$$

where $G(\rho_{\text{ID}}) \triangleq -(\frac{1}{c}f_{\text{LC}}^* + BR_{\text{U}}^*)$ is nonconvex and nondifferentiable. We can see that $G(\rho_{\text{ID}})$ is an increasing function with respect to ρ_{ID}. Also, for a feasible set $\mathcal{S} \triangleq \{(\rho_{\text{ID}},\omega) \mid \omega + G(\rho_{\text{ID}}) \le 0,\ 0 \le \rho_{\text{ID}} \le 1,\ \omega \ge 0\} \subset \mathbb{R}_+^2$, we can check that $\mathcal{S}$ is normal, namely, if $\mathbf{s}_1 \in \mathcal{S}$, then the normal set $\mathcal{S}$ includes all $\mathbf{s}_2$ such that $\mathbf{0} \le \mathbf{s}_2 \le \mathbf{s}_1$, and $F_3(\rho_{\text{ID}},\omega)$ is an increasing function over $\mathcal{S}$. Therefore, the optimal solution of (P″) is determined at the upper boundary of $\mathcal{S}$, i.e., $\omega + G(\rho_{\text{ID}}) = 0$.

Algorithm 1: Joint Optimization Algorithm for (P).

Initialize $F_3(\mathbf{v}^{(0)}) = -\infty$, and $i = 1$.
Repeat
  Select $\mathbf{v}^{(i)} = \text{argmax} F_3(\mathbf{v}|\mathbf{v} \in \mathcal{V}^{(i-1)})$.
  Compute $\pi(\mathbf{v}^{(i)}) = \alpha \mathbf{v}^{(i)}$ which holds equality in (27).
  Update $\mathcal{V}^{(i)}$ from (30) and let $i \leftarrow i + 1$.
Until convergence
Determine the optimal solution as $\rho_{\text{ID}}^* = \rho_{\text{ID}}^{(i)}$.

As a result, (P′′) can be handled by the polyblock outer approximation framework to attain the optimal solution [23]. A polyblock defined by the union of rectangles is given as

$$\mathcal{P}(\mathcal{V}) \triangleq \bigcup_{\mathbf{v} \in \mathcal{V}} \{\mathbf{p} | \mathbf{0} \leq \mathbf{p} \leq \mathbf{v}\} \subset \mathbb{R}_+^2, \tag{29}$$

where $\mathcal{V} \subset \mathbb{R}_+^2$ is a set of the vertices of $\mathcal{P}(\mathcal{V})$. In the proposed algorithm, we first initialize the vertex set as $\mathcal{V}^{(0)} = \{\mathbf{v}^{(0)}\}$ where $\mathbf{v}^{(0)} = (\rho_{\text{ID}}^{(0)}, \omega^{(0)})$ such that $\rho_{\text{ID}}^{(0)} = 1$ and $\omega^{(0)} = -G(0)$, and then the normal set $\mathcal{S}$ is a subset of $\mathcal{P}(\mathcal{V}^{(0)})$. At the i-th iteration, the algorithm choose a vertex $\mathbf{v}^{(i)} = (\rho_{\text{ID}}^{(i)}, \omega^{(i)})$ over $\mathcal{P}(\mathcal{V}^{(i-1)})$ which maximizes the objective, i.e., $\mathbf{v}^{(i)} = \text{argmax} F_3(\mathbf{v}|\mathbf{v} \in \mathcal{V}^{(i-1)})$. Note that since $F_3(\mathbf{v}^{(i)})$ is a monotonic function with respect to $\mathbf{v}^{(i)}$, $\mathbf{v}^{(i)}$ can be obtained at one of the vertices in $\mathcal{V}^{(i-1)}$.

Then, the algorithm updates a new vertex set $\mathcal{V}^{(i)}$ which satisfies $\mathcal{S} \subset \mathcal{P}(\mathcal{V}^{(i)}) \subset \mathcal{P}(\mathcal{V}^{(i-1)})$. Specifically, to generate new vertices of $\mathcal{P}(\mathcal{V}^{(i)})$, we denote $\pi(\mathbf{v}^{(i)})$ as the projection of $\mathbf{v}^{(i)}$ onto the upper boundary of $\mathcal{S}$. Since $\mathcal{S}$ is normal, we can obtain $\pi(\mathbf{v}^{(i)})$ by letting $\pi(\mathbf{v}^{(i)}) = \alpha^{(i)} \mathbf{v}^{(i)}$ and calculating $\alpha^{(i)}$ for $0 < \alpha^{(i)} < 1$ using the one-dimensional bisection search method which is a low complexity algorithm. Accordingly, for a vertex set $\mathcal{V}^- = \{\mathbf{v} \in \mathcal{V}^{(i-1)} | \mathbf{v} > \pi(\mathbf{v}^{(i)})\}$, the new vertex set is updated by

$$\mathcal{V}^{(i)} = \bar{\mathcal{V}}^{(i-1)} \cup \{(\alpha^{(i)} \rho_{\text{ID}}^{(i)}, v_2), (v_1, \alpha^{(i)} \omega^{(i)}) | (v_1, v_2) \in \mathcal{V}^-\}, \tag{30}$$

where $\bar{\mathcal{V}}^{(i-1)} = \mathcal{V}^{(i-1)} \setminus \mathcal{V}^-$.

Repeating the iterative procedure, the polyblock $\mathcal{P}(\mathcal{V}^{(i)})$ reaches $\mathcal{S}$. Therefore, from $\pi(\mathbf{v}^{(i)}) \in \mathcal{S}$ and $\pi(\mathbf{v}^{(i)}) = \alpha^{(i)} \mathbf{v}^{(i)}$, it can be checked that $F_3(\pi(\mathbf{v}^{(i)})) \leq F_3(\mathbf{v}^*) \leq F_3(\mathbf{v}^{(i)})$ where $\mathbf{v}^* \triangleq (\rho_{\text{ID}}^*, \omega^*)$ denotes the optimal solution of (P′′). Also, since $\mathbf{v}^{(0)} \geq \mathbf{v}^{(1)} \geq \ldots \geq \mathbf{v}^{(i)}$ and $\mathbf{v}^{(i)}$ is bounded by $\mathbf{v}^*$, the convergence of the proposed algorithm is guaranteed [23]. As a result, we can conclude that $\pi(\mathbf{v}^{(i)})$ finally converges to $\mathbf{v}^*$, and thus $\rho_{\text{ID}}^{(i)}$ also converges to the optimal ρ_{ID}^*. The overall procedure of the proposed algorithm for solving (P) is summarized in Algorithm 1.

IV. Numerical Results

In this section, we evaluate the performance of the proposed algorithm by numerical results with $N_{\text{rec}} = 4$. The path-loss exponent is set to $l = 3.5$ and it is assumed that $|\bar{h}_i|$ follows a normalized Rician distribution with the 3 dB Rician factor. We set the noise variance and the reference path-loss as $\sigma^2 = -100$ dBm and $g_i = -30$ dB, respectively. The system bandwidth and the number of required CPU cycles per bit are fixed as $B = 312.5$ kHz and $c = 100$, respectively [4]. In addition, the maximum transmission power and the computation frequency of the device are given by $P_{\text{U}}^M = 20$ dBm and $f_{\text{LC}}^M = 900$ MHz, respectively, and κ is given as $\kappa = 10^{-29}$. The constants related to the nonlinear rectifier are set to $a = 47083$, $b = 2.9 \times 10^{-6}$, and $M_{\text{max}} = 9.079 \times 10^{-6}$W [19], [21].

In Fig. 2, the latency optimized by the proposed algorithm for $X_{\text{L}} = X_{\text{C}} = 10$ kbits, $d_D = 5$ m with respect to d_U is illustrated. The transmission power of the H-AP is set to $P_{\text{D}} = 40$ dBm. To compare the performance, we also simulate the following baseline schemes.

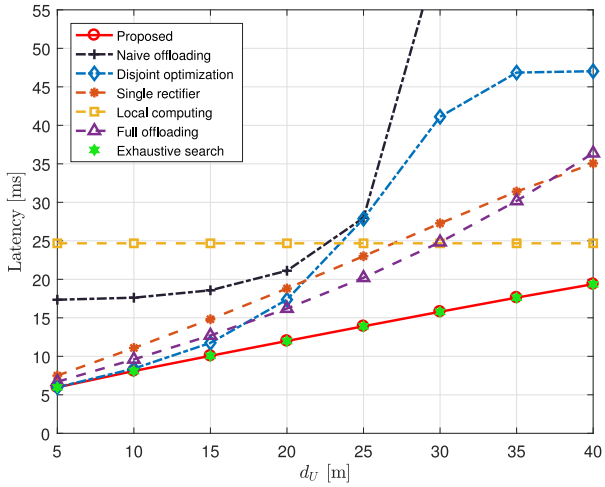

Fig. 2. Latency with respect to the distance between a device and a server.

- *Local computing:* The data offloading ratio is fixed as $\beta = 0$. Similar to the proposed algorithm, for a given ρ_{ID}, the EH power splitting ratio $\{\rho_n\}$ is optimized from (14) and the corresponding local computing frequency f_{LC} is obtained from a convex problem. Then, the optimal ID power splitting ratio ρ_{ID} is calculated from the polyblock outer approximation.
- *Full offloading:* The data offloading ratio is fixed as $\beta = 1$. Then, the remaining procedure is the same as the local computing scheme.
- *Single rectifier:* For $N_{rec} = 1$, the latency is optimized by the proposed algorithm.
- *Naive offloading:* The EH power splitting ratio $\{\rho_n\}$ is optimized based on an iterative algorithm in [20] for a given $\rho_{\text{ID}} = \frac{1}{1+N_{\text{rec}}}$. Then, fixing the data offloading ratio as $\beta = \frac{1}{2}$, the corresponding local computing frequency f_{LC} and the data offloading power P_U are obtained from (P) in the manuscript.
- *Disjoint optimization:* In this scheme, the EH power splitting ratio $\{\rho_n\}$, the local computing frequency f_{LC} and the data offloading power P_U are optimized from the algorithms in [20] and [2]. Specifically, $\{\rho_n\}$ is first optimized by the algorithm in [20] after determining ρ_{ID}. Then, under the available energy constraint, the data offloading latency optimization is computed by the algorithm in [2].
- *Exhaustive search:* The optimal solution of the problem is obtained by the exhaustive search.

First, we can check that the proposed system outperforms the local computing and full offloading systems. As d_U increases, the performance gain of the proposed system over full offloading scheme becomes larger. On the other hand, the gap between the proposed system and the local computing scheme gets smaller as d_U decreases. With these results, we can infer that applying the proposed partial data offloading strategy can bring performance enhancements compared to conventional schemes. Although the harvested energy is optimized, it can be checked that the latency of the naive offloading increases drastically without the optimization of the MEC operation. In addition, it is observed that the latency gap between the proposed joint optimization and the disjoint optimization becomes larger as d_U decreases.

Fig. 3 illustrates the data offloading ratio for the system configurations presented in Fig. 2. It can be seen that due to the separated optimization of the energy harvesting and the data execution operations, the disjoint optimization scheme does not efficiently utilize the computation resource of the server when d_U is large. In contrast, the proposed scheme actively performs data offloading even when the server is far away from the device. Based on these results, we can deduce that the maximization of the harvested energy at the device is crucial for the latency minimization of the data execution as well as the downlink SWIPT, and thus, the joint optimization of the EH and edge computing

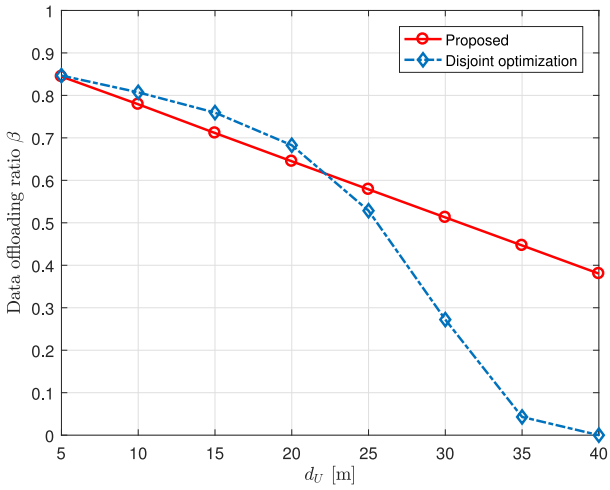

Fig. 3. Data offloading ratio with respect to the distance between a device and a server.

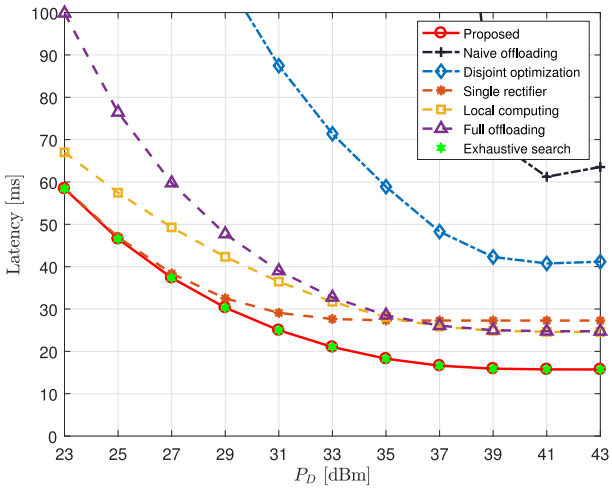

Fig. 4. Latency with respect to the transmission power of H-AP.

operations is important to fully exploit the proposed multiple rectifier structure in the wireless powered MEC network.

Fig. 4 exhibits the latency of various systems for $d_D = 5$ m and $d_U = 30$ m with respect to the transmission power of H-AP P_{D}. We can check that the proposed algorithm outperforms other baseline schemes regardless of P_{D}, and the latency optimized by the proposed algorithm exhibits at least a 50% gain when P_{D} is high. Also, it is observed that the performance gap between the proposed scheme and the single rectifier scheme is negligible when P_{D} is low, since the optimal EH power splitting ratio $\{\rho_n^*\}$ follows the single rectifier solution. On the other hand, the gap grows with P_{D} since the optimal $\{\rho_n^*\}$ is assigned to more than one rectifier for avoiding the operation in the saturation region of each rectifier. We can conclude that the joint optimization of the power splitting ratio as well as the local computing frequency and the data offloading power of multiple rectifier receivers is critical for the proposed MEC network.

REFERENCES

[1] Y. Mao, C. You, J. Zhang, K. Huang, and K. B. Letaief, "A survey on mobile edge computing: The communication perspective," *IEEE Commun. Surv. Tut.*, vol. 19, no. 4, pp. 2322–2358, 2017.

[2] Y. Wang, M. Sheng, X. Wang, L. Wang, and J. Li, "Mobile-edge computing: Partial computation offloading using dynamic voltage scaling," *IEEE Trans. Commun.*, vol. 64, no. 10, pp. 4268–4282, Oct. 2016.

[3] Y. Dai, D. Xu, S. Maharjan, and Y. Zhang, "Joint computation offloading and user association in multi-task mobile edge computing," *IEEE Trans. Veh. Technol.*, vol. 67, no. 12, pp. 12 313–12325, Dec. 2018.

[4] H. Xing, L. Liu, J. Xu, and A. Nallanathan, "Joint task assignment and resource allocation for D2D-enabled mobile-edge computing," *IEEE Trans. Commun.*, vol. 67, no. 6, pp. 4193–4207, Jun. 2019.

[5] N. Kiran, C. Pan, S. Wang, and C. Yin, "Joint resource allocation and computation offloading in mobile edge computing for SDN based wireless networks," *J. Commun. Netw.*, vol. 22, no. 1, pp. 1–11, Feb. 2020.

[6] M. Huang, W. Liu, T. Wang, A. Liu, and S. Zhang, "A Cloud-MEC collaborative task offloading scheme with service orchestration," *IEEE Internet Things J.*, vol. 7, no. 7, pp. 5792–5805, Jul. 2020.

[7] Z. Ning, X. Wang, and J. Huang, "Mobile edge computing-enabled 5G vehicular networks: Toward the integration of communication and computing," *IEEE Trans. Veh. Mag.*, vol. 14, no. 1, pp. 54–61, Mar. 2019.

[8] S. Bi, C. K. Ho, and R. Zhang, "Wireless powered communication: Opportunities and challenges," *IEEE Commun. Mag.*, vol. 53, no. 4, pp. 117–125, Apr. 2015.

[9] M. Ashraf, S. Kang, and I. Lee, "Harvested energy maximization in wireless peer discovery systems," *IEEE Commun. Lett.*, vol. 23, no. 5, pp. 934–937, May 2019.

[10] H. Lee, H. Kim, K. Lee, and I. Lee, "Asynchronous designs for multiuser MIMO wireless powered communication networks," *IEEE Syst. J.*, vol. 13, no. 3, pp. 2420–2430, Sep. 2019.

[11] J. Xu, L. Liu, and R. Zhang, "Multiuser MISO beamforming for simultaneous wireless information and power transfer," *IEEE Trans. Signal Process.*, vol. 62, no. 18, pp. 4798–4810, Sep. 2014.

[12] L. Liu, R. Zhang, and K. Chua, "Wireless information and power transfer: A dynamic power splitting approach," *IEEE Trans. Commun.*, vol. 61, no. 9, pp. 3990–4001, Sep. 2013.

[13] B. Clerckx, R. Zhang, R. Schober, D. W. K. Ng, D. I. Kim, and H. V. Poor, "Fundamentals of wireless information and power transfer: From RF energy harvester models to signal and system designs," *IEEE J. Sel. Areas Commun.*, vol. 37, no. 1, pp. 4–33, Jun. 2019.

[14] J. Kim, B. Clerckx, and P. D. Mitcheson, "Experimental analysis of harvested energy and throughput trade-off in a realistic SWIPT system," in *Proc. IEEE Wireless Power Transfer Conf.*, 2019, pp. 1–5.

[15] A. I. Akin, I. Stupia, H. Mirghasemi, and L. Vandendorpe, "On the performance of SWIPT MEC systems in the presence of spatially correlated shadowing," in *Proc. IEEE Glob. Commun. Conf.*, 2020, pp. 1–6.

[16] F. Wang, J. Xu, X. Wang, and S. Cui, "Joint offloading and computing optimization in wireless powered mobile-edge computing systems," *IEEE Trans. Wireless Commun.*, vol. 17, no. 3, pp. 1784–1797, Mar. 2018.

[17] H. Zheng, K. Xiong, P. Fan, Z. Zhong, and K. B. Letaief, "Fog-assisted multiuser SWIPT networks: Local computing or offloading," *IEEE Internet Things J.*, vol. 6, no. 3, pp. 5246–5264, Jun. 2019.

[18] F. Zhou, Y. Wu, R. Q. Hu, and Y. Qian, "Computation efficiency in a wireless-powered mobile edge computing network with NOMA," in *Proc. IEEE Int. Conf. Commun.*, 2019, pp. 1–7.

[19] E. Boshkovska, D. W. K. Ng, N. Zlatanov, and R. Schober, "Practical non-linear energy harvesting model and resource allocation for SWIPT systems," *IEEE Commun. Lett.*, vol. 19, no. 12, pp. 2082–2085, Dec. 2015.

[20] G. Ma, J. Xu, Y. Zeng, and M. R. V. Moghadam, "A generic receiver architecture for MIMO wireless power transfer with nonlinear energy harvesting," *IEEE Signal Process. Lett.*, vol. 26, no. 2, pp. 312–316, Feb. 2019.

[21] X. Liu, Z. Li, and C. Wang, "Secure decode-and-forward relay SWIPT systems with power splitting schemes," *IEEE Trans. Veh. Technol.*, vol. 67, no. 8, pp. 7341–7354, Aug. 2018.

[22] J. Kim, H. Lee, S. Park, and I. Lee, "Minimum rate maximization for wireless powered cloud radio access networks," *IEEE Trans. Veh. Technol.*, vol. 68, no. 1, pp. 1045–1049, Jan. 2019.

[23] H. Tuy, "Monotonic optimization: Problems and solution approaches," *SIAM J. Optim.*, vol. 11, no. 2, pp. 464–494, Nov. 2000.

[24] S. Boyd and L. Vandenberghe, *Convex Optimization*. Cambridge, U.K.: Cambridge Univ. Press, 2004.